의학박사 학위논문

# Therapeutic effects of mesenchymal stem cells for diabetic detrusor underactivity in rat model

당뇨병성 저활동성 방광 질환 쥐 모델에서 줄기세포 치료의 효과

울 산 대 학 교 대 학 원

의 학 과

신 정 현

# 당뇨병성 저활동성 방광 질환 쥐 모델에서 줄기세포 치료의 효과

지도교수 주 명 수

이 논문을 의학박사 학위논문으로 제출함

**2019 년 2 월**

울 산 대 학 교 대 학 원

의 학 과

신 정 현

신정현의 의학박사학위 논문을 인준함

심사위원장 박 형 근 (인)

심사위원 주 명 수 (인)

심사위원 송 상 훈 (인)

심사위원 신 동 명 (인)

심사위원 오 승 준 (인)

울 산 대 학 교 대 학 원

2019 년 2 월

# ABSTRACT


**Background**

Detrusor underactivity or underactive bladder has limited pharmacological treatment and surgical intervention. Diabetes, a global public health problem, is one of the risk factors. We aimed to establish a rat model with diabetic detrusor underactivity and evaluate therapeutic effects of multipotent mesenchymal stem cells (M-MSCs) derived from human embryonic stem cells (hESCs).

**Materials and methods**

8-week-old female Sprague-Dawley rats were used to create diabetic model and M-MSCs were prepared by differentiation of human embryonic stem cell. The optimal dose and timing for further experiment were established by comparing the mortality rate with different dosage of streptozotocin (STZ, 50mg/kg vs. 60mg/kg) and longitudinal change in bladder function (14 days vs. 21 days vs. 28 days). Accordingly, rats were fasted overnight (>12hours) and STZ 50mg/kg was injected intraperitoneally. Blood sample was acquired to measure serum

glucose level three days later. Rats with plasma glucose level <200mg/dL were excluded from the study. Three weeks (21 days) after induction, diabetic model created with 50mg/kg of STZ was divided into five groups: sham (n=10), DM (n=10), 250k M-MSC (n=10), 500k M-MSC (n=10) and 1,000k M-MSC (n=10). Three different dose of M-MSCS were directly injected into the submucosal layer at anterior wall or dome of the bladder with 26-gauge needle. One week after the injection, awake cystometry and immunohistochemical staining were performed.

**Results**

STZ group had significantly longer micturition interval (106.3±1.47 vs. 55.47±0.52 sec; $p<0.001$), larger residual urine (0.25±0.01 vs. 0.12±0.03 mL; $p<0.005$) and decreased micturition pressure (23.07±2.05 vs. 56.99±0.64 $cmH_2O$; $p<0.001$) on awake cystometry than sham group. Immunohistochemical staining showed increased apoptosis of muscle tissue in STZ group. However, M-MSC injection ameliorated bladder dysfunction and muscle layer was restored even in suboptimal dosage. Under confocal imaging, M-MSCs were mostly observed at stroma in muscle layer of the bladder.

**Conclusions**

We established diabetic DUA model with STZ injection in rats. Transplantation of human ESCs derived M-MSC ishowed the possibility of therapeutic effect on established models. It is estimated that M-MSCs differentiate into myocyte and perivascular structures. Further study to identify differentiation and reveal the exact mechanism of M-MSCs is needed.

**Keywords:** Detrusor underactivity, diabetes mellitus, streptozotocin, mesenchymal stem cell

# CONTENTS

# LIST OF FIGURES

# LIST OF ABBREVIATIONS

**DUA** detrusor underactivity

**UAB** underactive bladder

**DM** diabetes mellitus

**M-MSC** multipotent mesenchymal stem cell

**IC** interstitial cystitis

**STZ** streptozotocin

**hESC** human embryonic stem cell

**ADSC** adipose tissue derived mesenchymal stem cell

**NGF** nerve growth factor

**VEGF** vascular endothelial growth factor

# INTRODUCTION

Detrusor underactivity (DUA) is a urodynamic diagnosis defined as "a contraction of reduced strength and/or duration, resulting in prolonged bladder emptying and/or failure to achieve complete bladder emptying within a normal time span" by International Continence Society.[1] The accurate prevalence of DUA is not known, as the diagnosis is based on invasive pressure flow studies, but it is assumed to have a higher incidence in elderly.[2] DUA might lead to both storage and voiding lower urinary tract symptoms, recurrent urinary tract infection and urinary retention, resulting in deterioration of patients' quality of life.[3] Recently, a concept of underactive bladder (UAB) has been developed for the symptom-based correlation of DUA.[4]

DUA or UAB might result from various pathological processes that could be classified as idiopathic, neurogenic, or myogenic.[5] Idiopathic DUA is defined as 'free of evident neuropathy, functional or anatomical bladder obstruction and shows low or no detrusor pressure combined with low maximum flow and large post-void residual, or urinary retention'.[6] Neurogenic DUA is due to any alteration of neural control mechanisms.[7]

Myogenic DUA may result from the alteration in ion storage and/or exchange, energy generation and degenerative change of bladder smooth muscle.[8] However, there is a lack of understanding in natural course and underlying pathophysiological mechanisms of DUA.

Aging, neurological deficits, diabetes mellitus (DM), persistent bladder outlet obstruction with consequent detrusor hypertrophy are suggested risk factors for DUA.[9] Above all, DM is one of the most important global public health challenges of twenty-first century of which prevalence is estimated up to 10%.[10] DM is a predisposing factor for various complications and diabetic cystopathy has incidence of 50% in diabetic patients.[11] Duration, severity and adequate control of the disease affects the severity of diabetic cystopathy.[12] Exact pathogenesis of diabetic cystopathy is unclear, but it is suggested that myogenic dysfunction of detrusor leads to decreased contractility and DM-associated autonomic neuropathy decreases bladder sensation.[13,14] Treatment options for DUA can be subcategorized into the augmentation of detrusor contractility, reducing bladder outlet resistance and circumvention of existing problems.[15] However, effective pharmacological treatment or surgical intervention

of DUA is lacking[16] and one study showed that 84% of DUA patients who initially chose conservative management remained untreated at nearly 14-year follow-up.[17]

Stem cells undergo self-renewal and simultaneously give rise to differentiation-related progenitors to replace damaged cells.[18] Therapeutic potential of stem cell has been studied in various bladder dysfunction animal models.[19] Previously, we have demonstrated the therapeutic effects of multipotent mesenchymal stem cells (M-MSCs) derived from human embryonic stem cells (hESCs) in different interstitial cystitis (IC) rat models.[20-22] Regarding DUA, chronic ischemia by bilateral iliac artery ligation or hyperlipidemia, cryoinjury or pelvic injury models were used and there has been only one stem cell study with diabetic DUA model.[23] Commonly used diabetic rat model is streptozotocin (STZ) model, as a model can be created with single injection.[24] In this study, we aimed to create our diabetic DUA model with STZ and evaluate the therapeutic effects of M-MSCs.

# MATERIALS AND METHODS

**1. Culture of hESC (human embryogenic stem cell)-derived M-MSC**

Human H9 ESCs were differentiated into M-MSCs following previously described protocols.[25,26] Established M-MSCs were cultured in EGM2-MV medium (Lonza, San Diego, CA, USA) on rat tail collagen type I (Sigma-Aldrich, St. Louis, MO) coated plates in a humidified and heated atmosphere of 5% $CO_2$ at 37°C. All M-MSCs were expanded less than ten passages to ensure multipotency. GFP expression was established by infection of a GFP expressing lentivirus, which was produced as previously described.[20]

**2. Animal model and study design**

All experimental animal procedures were approved by the institutional animal care and use committee. Female Sprague-Dawley rats (8-week-old) were used in this study. STZ (Sigma Chemical Company, St. Louis, MO, USA) was used to induce type I diabetes.

To find out optimal dose of STZ for the diabetic model, rats were injected with different dosage of STZ (50 or 60 mg/kg body weight in 0.1M citrate buffer, Ph 4.5, n = 10, respectively) intraperitoneally after overnight fasting. Blood glucose level was measured 72

hours after with samples obtained by tail prick. Rats with glucose level higher than 200 mg/dL (16.7 mmoL/L) were selected as diabetic rats. Survival of rats in each group was identified four weeks after diabetes induction. Then, we performed awake cystometry to evaluate bladder function. STZ concentration was selected based on the survival rate and presence of DUA (**Figure 1A**).

Next, we observed longitudinal change of bladder function to select optimal timing for stem cell injection. In diabetic model created with optimal STZ concentration, we evaluated bladder functions 14, 21 and 28 days later (n = 3, respectively) with awake cystometry (**Figure 1B**).

Finally, we injected different dosages of M-MSCs to figure out therapeutic effect and suboptimal dosage. After an overnight fast, rats were intraperitoneally injected with STZ (50 mg/kg body weight in 0.1M citrate buffer, Ph 4.5) dissolved in citrate acid buffer solution. The remaining rats were injected with an equivalent volume of citrate buffer solution and served as controls. Rats with plasma glucose level higher than 200 mg/dL (16.7 mmoL/L) three days later were selected as diabetic rats. Three weeks after diabetes induction, the rats

were anesthetized with 0.2 ml tiletamine (Zoletil1®, Virbac Laboratories, Carros, France) and divided into five groups: nondiabetic controls (Con, n = 10); diabetic rats injected with PBS (diabetes mellitus [DM], n = 10); diabetic rats a single administration of the indicated dose (0.25, 0.5, and $1x10^6$ cells/200μL, n = 10) of M-MSCs into the outer-layer (serosa) of the bladder. The therapeutic effect of stem cells was examined with awake cystometry and histological 1 week after stem cells injection. Body weight and blood glucose levels were measured and recorded weekly during this study. Fasting and postprandial blood glucose levels were determined with an Accu-check blood glucose meter (Roche Diagnostics) before the rats were killed (**Figure 1C)**.

**Figure 1. Schematic diagram of animal model establishment and the study design**

(A) Optimal dosage (B) Optimal timing (C) study design

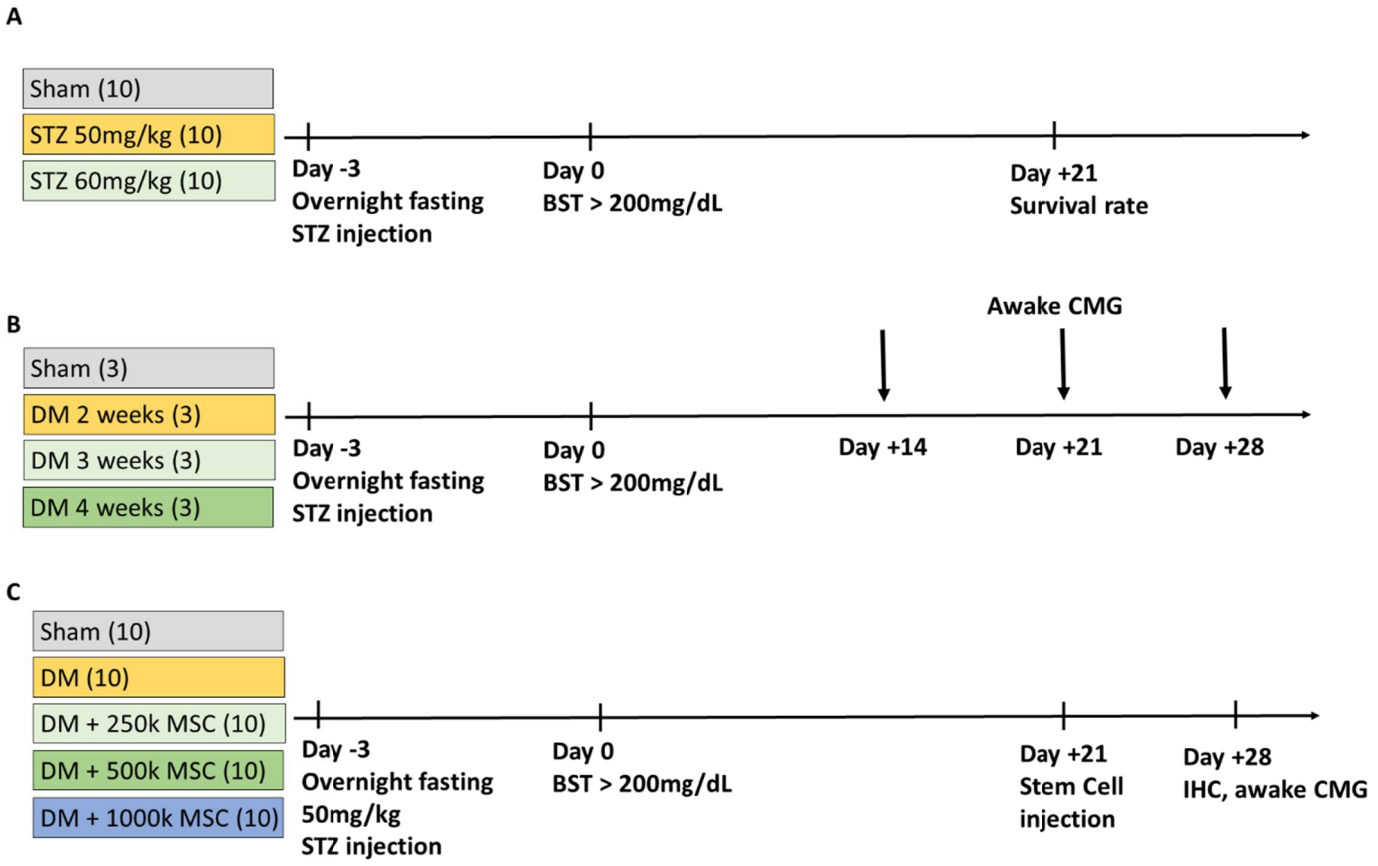

**3. Evaluation of Bladder Function and Tissue Preparation**

Cystometric evaluation was performed in the awake state with unrestrained animals in metabolic cages. Three days prior to the cystometrogram, intravesical pressure (IVP) and intra-abdominal pressure (IAP) recordings were performed. The urethra was approached by using a PE-50 catheter (Clay Adams, Parsippany, NJ) connected to a pressure transducer (Research Grade Blood Pressure Transducer; Harvard Apparatus, Holliston, MA, USA) and a microinjection pump (PHD22/2000 pump; Harvard Apparatus). The voiding volumes were recorded by means of a fluid collector connected to a force displacement transducer (Research Grade Isometric Transducer; Harvard Apparatus) as normal saline was infused into the bladder at a rate of 0.4 ml/min. The IVP, IAP and voiding volumes were recorded continuously using Acq Knowledge 3.8.1 software and an MP150 data acquisition system (Biopac Systems, Goleta, CA, USA) at a sampling rate of 50 Hz. The mean values from three reproducible voiding cycles using individual animals were used for evaluation. Criteria for counting non-voiding contraction (NVC) was when the increments of IVP exceeded 15 $cmH_2O$ from baseline without expelled urine. BP (bladder pressure) was defined as the lowest

bladder pressure during filling, MP (micturition pressure) as the maximum bladder pressure during the micturition cycle, MV (micturition volume) as the urine volume of expelled urine, and RV (residual volume) as the urine volume remaining following voiding. In agreement with prior work, MI (micturition interval) was defined as the interval between micturition contractions and BC (bladder capacity) was defined as MV + RV. The mean values from three reproducible micturition cycles were evaluated with five individual animals (n=5). After evaluation of voiding function, the bladder of each rat was harvested. Half of each bladder was cryopreserved in liquid nitrogen for RNA extraction. The remaining half was fixed in 4% buffered formalin and embedded in paraffin prior to sectioning followed by immunohistochemical staining.

**4. Histological analysis**

After 24-hours fixation in 4% paraformaldehyde, each bladder was embedded in paraffin, cut on a microtome into 3-μm-thick slices, affixed to slides, and stained with hematoxylin and eosin. The histological quantification of smooth muscle, tissue fibrosis, apoptosis and neurofilament was assessed by immunostaining of Masson's trichrome

staining (Junsei Chemical, Tokyo, Japan), TUNEL staining (1 684 795; Roche, Mannheim, Germany) and neurofilament 200 (N200; Abcam, Cambridge, MA, USA) staining. The nuclei were counterstained with 4',6-diamino-2-phenylindole (DAPI). Three randomly chosen representative areas were selected from each slide for quantitative digital image analysis using Image Pro 5.0 software (Media-Cybernetics, Rockville, MD, USA).

**5. Organ bath study**

We performed organ bath study in sham (n = 5), DM (n = 5) and diabetic rats with single administration of M-MSCs ($1x10^6$ cells/200μL, n = 5). The bladders were cut into two strips with mucosa along the longitudinal axis. The strips were mounted in an organ bath system (Danish Myo Technology, Aarhus, Denmark) containing 15mL of Krebs buffer. Briefly, bladder strips were subjected to resting tension of 1g and allowed to stabilize for at least 60 minutes. Contractions were recorded as changes in tension from baseline in response to 60 mM KCl, carbachol (concentration from 3 nM to 100 mM), electrical field stimulation (EFS; 1,2,4,8,16 and 32 Hz ) and 1 mM ATP. All tissue responses were normalized to tissue weight in g. Drug concentrations are expressed as final

concentrations in the bath. Drugs and chemicals were obtained from Sigma.

**6. GFP staining**

$GFP^+$ M-MSCs in the bladder were tracked by staining samples with a rabbit polyclonal anti-GFP antibody (ab290; Abcam, Cambridge, MA, USA). Differentiation of $GFP^+$ cells into epithelial, stromal, endothelial, and perivascular cells was examined by staining samples with antibodies against E-cadherin (612130; clone 36; FITC-conjugated; BD Biosciences), vimentin (sc-6260; Santa Cruz Biotechnology), CD31 (sc-376764; Santa Cruz Biotechnology), respectively. To analyze the cellular properties of surviving M-MSCs, immunohistological analysis of bladder tissues was performed by multichannel scanning laser confocal imaging.

**7. Statistical analysis**

Data were reported as the mean ± standard error of the mean (SEM) and were analyzed by GraphPad Prism 6.0 software (GraphPad Software, La Jolla, CA). Differences and significance were verified by one-way or two-way ANOVA followed by Bonferroni post hoc tests. P-value less than 0.05 was considered statistically significant.

# Results

### Creation of DUA model

Survival of rats injected with different dosage of STZ is illustrated in Figure 2A. Rats with STZ (60 mg/kg body weight in 0.1M citrate buffer, pH 4.5) showed higher mortality than 50 mg/kg group (70% vs. 20%) on day 21. In awake cystometry, the diabetic model on day 14 showed no significant difference in general condition with the sham group. In addition, diabetic model on day 28 had no detrusor contraction and self-voiding (**Figure 2B**).

### Evaluation of bladder function with awake cystometry

To evaluate the functional improvement of bladder with a single administration of M-MSCs, we employed awake cystometry (**Figure 3A**). In comparison with animals in a sham-operated group (sham), STZ group exhibited irregular voiding patterns and increased micturition intervals (MI) (106.3±1.47 vs. 55.47±0.52 sec; $p<0.001$), micturition volume (MV) (0.45±0.03 vs. 0.25±0.02 mL; $p<0.001$), bladder capacity (BC) (0.68±0.01 vs. 0.38±0.01 mL; $p<0.001$), and residual volume (RV) (0.25±0.01 vs. 0.12±0.03 mL; $p<0.005$). STZ group also showed decreased micturition pressure (MP) (23.07±2.05 vs. 56.99±0.64 $cmH_2O$; $p<0.001$), and maximum pressure (23.82±2.06 vs. 57.16±0.64 $cmH_2O$; $p<0.001$). A single transplantation of $1\times10^6$ M-MSCs into the STZ + M-MSC group significantly ameliorated these defective voiding parameters. (**Figure 3B**)

**Figure 2. Establishment of animal model**

(A) Optimal dosage of MSC regarding survival rate (B) Optimal timing for stem cell injection

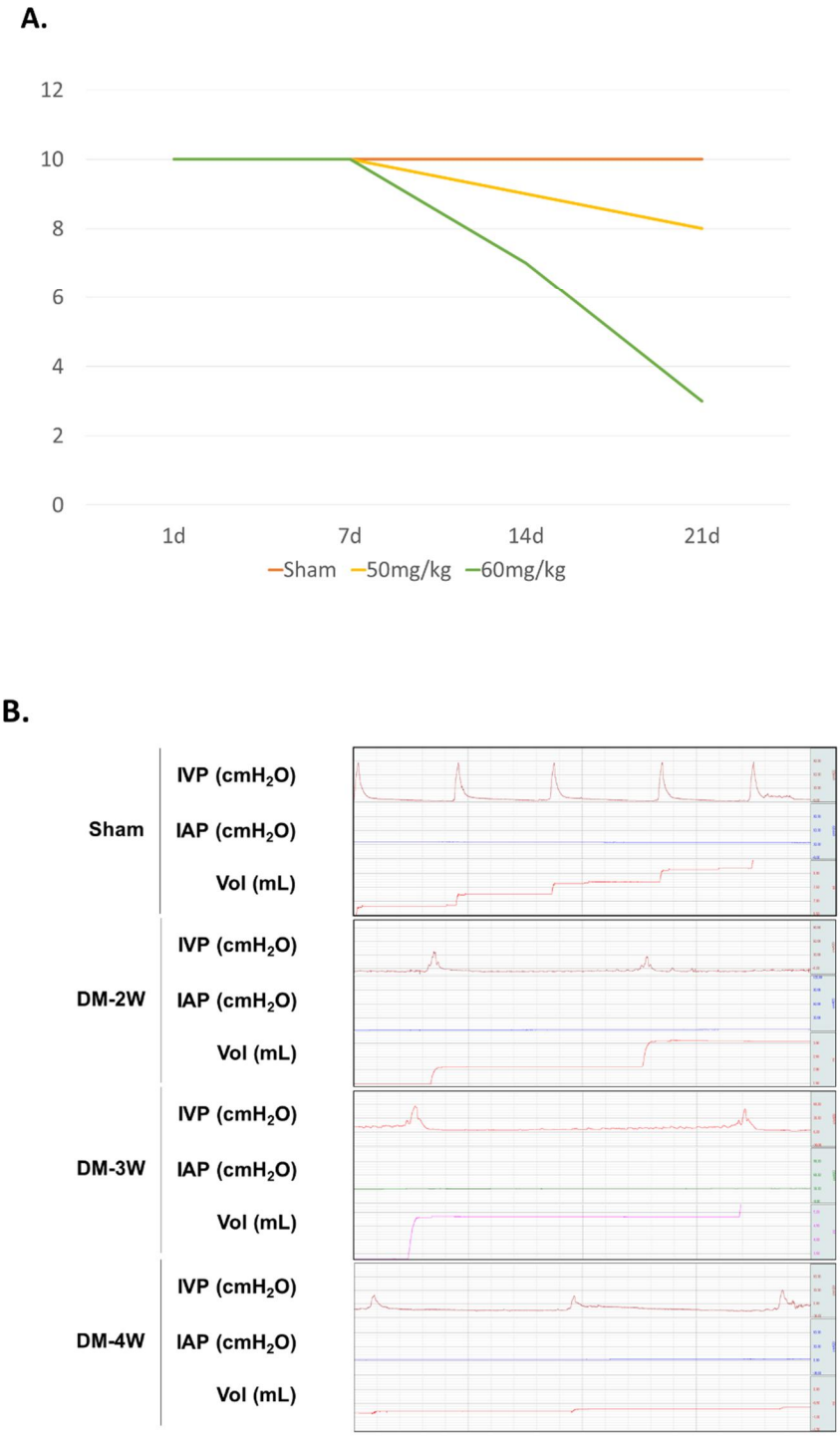

**Figure 3. M-MSCs injection ameliorated the bladder dysfunction in STZ rat mo del**

Representative awake cystometry results (B) quantitative voiding parameters. Data are presented as the mean ± SEM (from 5 independent animals in each group), *p < 0.05, **p < 0.01, ***p < 0.001 compared to the LPS-IC group; #p < 0.05, ##p < 0.001, ###p < 0.001 compared to the 1000 K group with Bonferroni post-test. IVP; intravesical pressure, IAP; intra-abdominal pressure. Sham: sham-operated.

**A.**

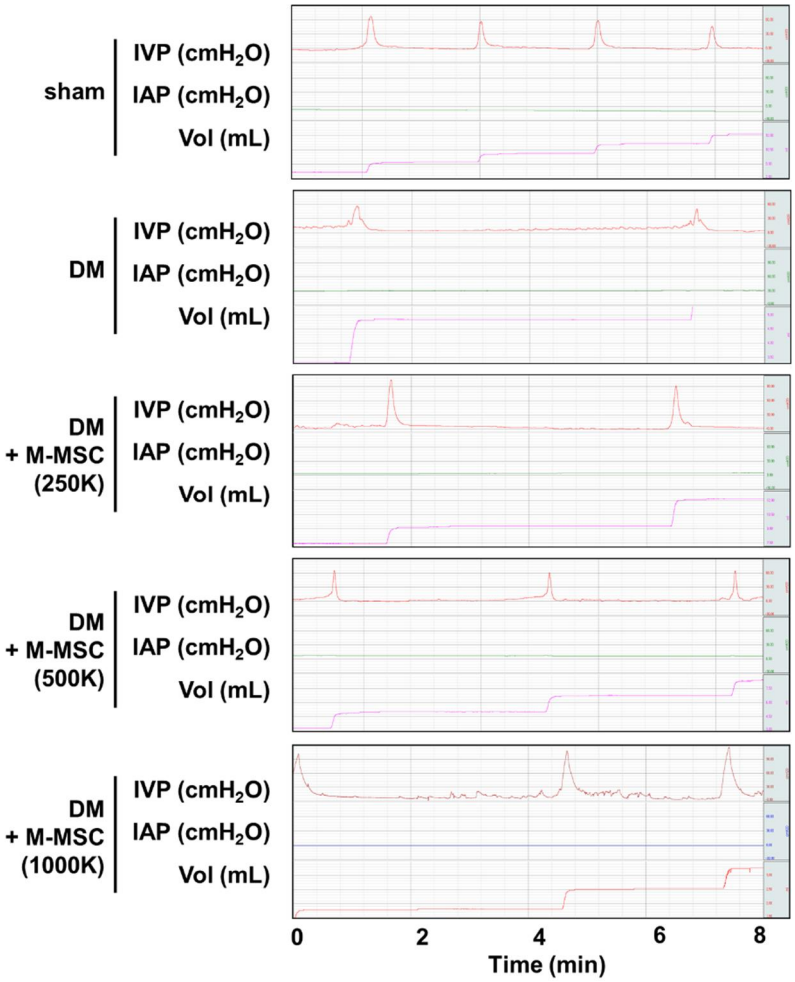

**B.**

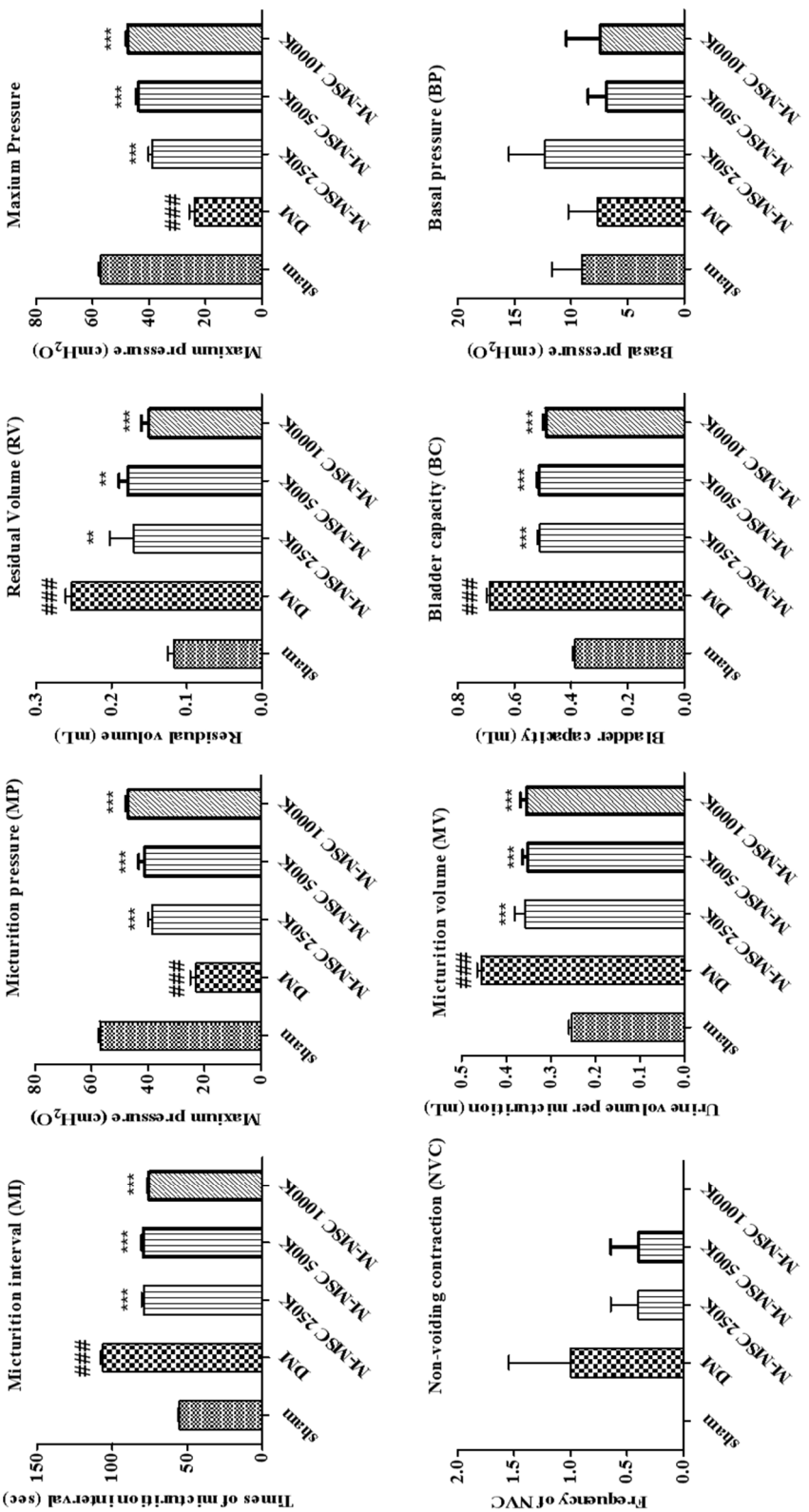
Micturition interval (MI)
Times of micturition interval (sec)
Micturition pressure (MP)
Maxium pressure (cmH2O)
Residual Volume (RV)
Residual volume (mL)
Maxium Pressure
Maxium pressure (cmH2O)
Non-voiding contraction (NVC)
Frequency of NVC
Micturition volume (MV)
Urine volume per micturition (mL)
Bladder capacity (BC)
Bladder capacity (mL)
Basal pressure (BP)
Basal pressure (cmH2O)
sham
DM
M-MSC 250K
M-MSC 500K
M-MSC 1000K

**Histological analysis of the effect of MSC therapy**

Compared with the sham-operated rats, the bladders of the STZ rat model presented smooth muscle atrophy and no significant difference in fibrosis with Masson's trichrome staining. Tissue apoptosis with markedly observed in terminal dUTP nick-end labeling (TUNEL)-stain. M-MSC administration significantly reversed the smooth muscle atrophy and apoptosis of STZ bladder. However, there was no difference in neurofilament between sham and DM group. (**Figure 4**).

**Organ bath study**

The contractile responses to 80 mM KCl, 1 mM ATP, frequency response to electrical field stimulation (EFS), concentration-response curve to carbachol (Cch) in the DM bladder strips were significantly lower than those in the control bladder strips. In the DM+M-MSC group, the contractile responses were significantly higher than those in the DM groups at the higher but not the lower frequencies (**Figure 5**).

**Figure 4. M-MSC therapy ameliorated histological abnormalities in STZ bladder.**

Hematoxylin and eosin (H & E) staining (i) (magnification ×200, scale bar = 100 μm), Masson's trichrome staining (ii) (magnification ×100, scale bar = 100 μm), TUNEL assay (iii) (magnification ×400, scale bar = 100 μm) and N200 staining (iv) (magnification ×100, scale bar = 100 μm) in bladder tissues of STZ rats 1 week after PBS injection or transplantation of M-MSCs at the indicated dosage (K = a thousand). Data are presented as the mean ± SEM, **p < 0.01, ***p < 0.001 compared to the LPS-IC group; #p < 0.05, ##p < 0.001, ###p < 0.001 compared to the 1000 K group with Bonferroni post-test.

sham
DM
DM + M-MSC (250K)
DM + M-MSC (500K)
DM + M-MSC (1000K)
H&E Staining
Masson-Trichrome Staining
TUNEL Staining
Mucosal layer
Muscular layer

**N200 Staining**

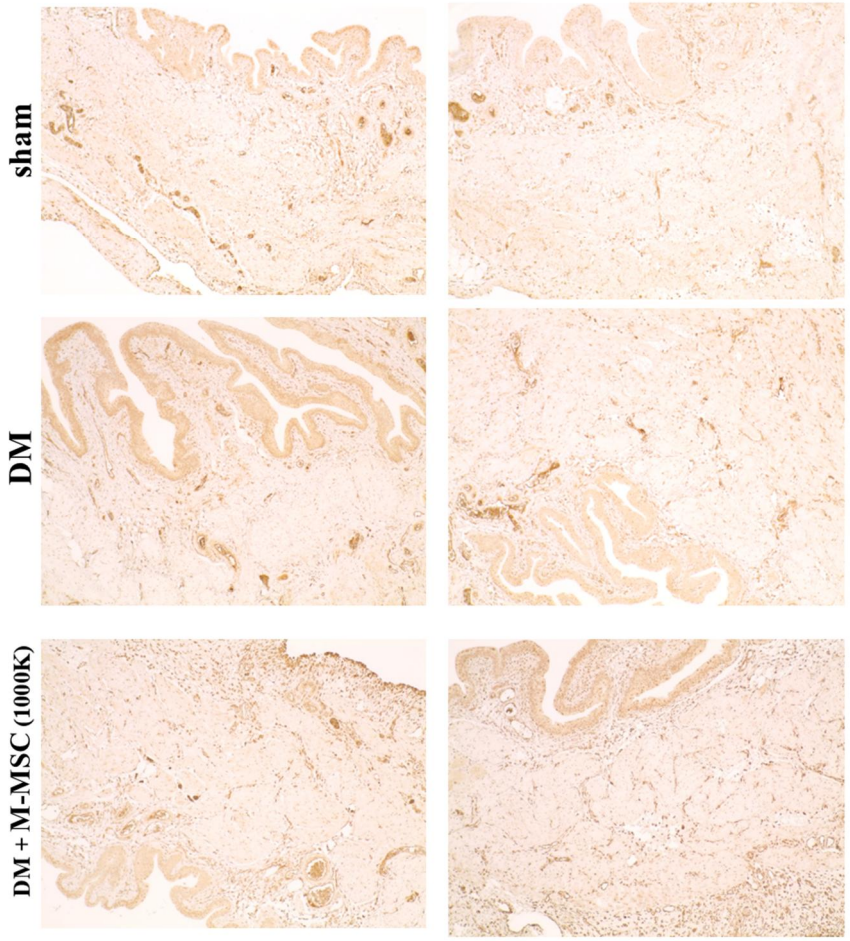

**Figure 5. Organ bath study**

Contractile response to 80 mM KCl, 1 mM ATP, frequency response to electrical field stimulation (EFS), concentration-response curve to carbachol (Cch) in control, DM and DM+M-MSC rats.

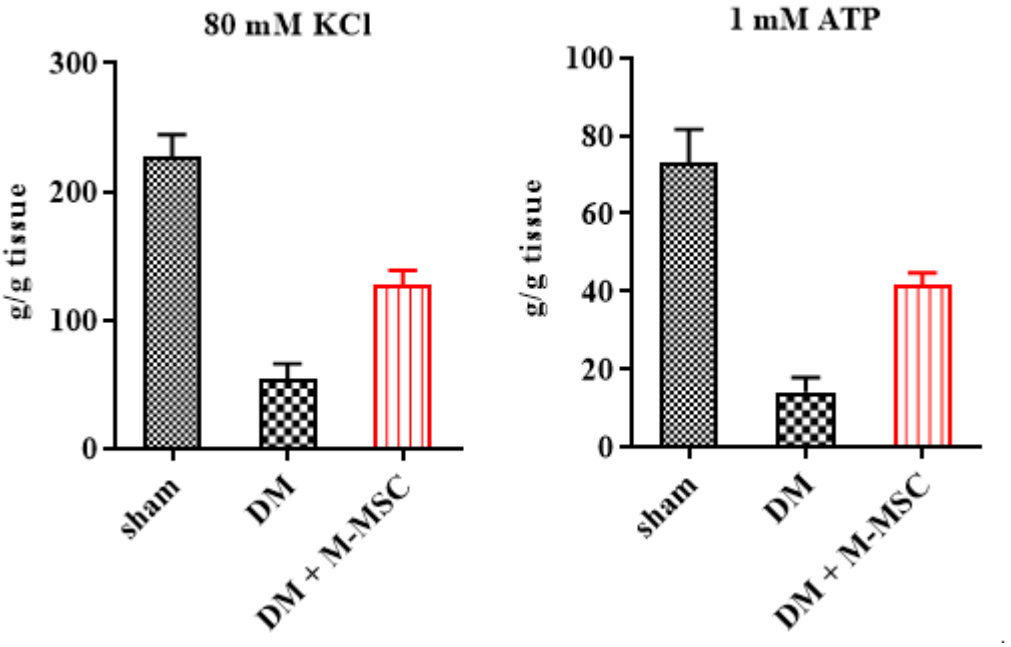

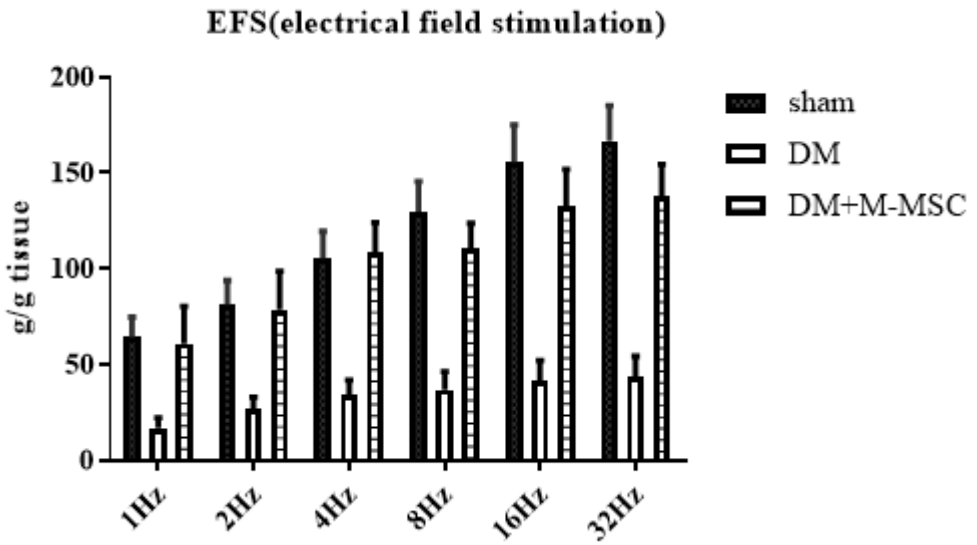
EFS(electrical field stimulation)
200
150
100
50
0
g/g tissue
1Hz
2Hz
4Hz
8Hz
16Hz
32Hz
sham
DM
DM+M-MSC

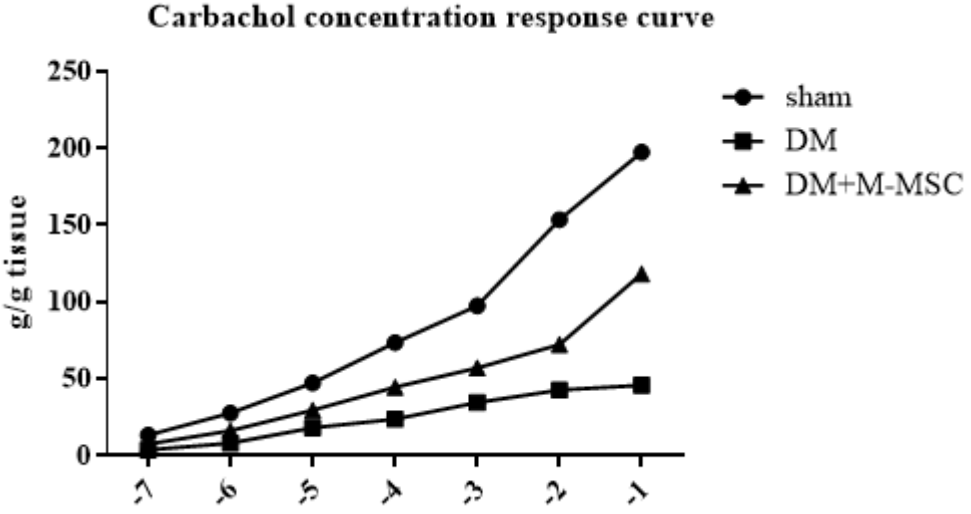
Carbachol concentration response curve
250
200
150
100
50
0
g/g tissue
-7
-6
-5
-4
-3
-2
-1
sham
DM
DM+M-MSC

**GFP staining, What M-MSCs differentiate into**

Engrafted cells, epithelial cells, stromal cells, and endothelial cells were detected based on expression of GFP, E-cadherin, vimentin, and CD31, respectively (Figure 6). At 7 DAT, many GFP+ cells were detected in the urothelium, lamina propria, and serosa. The majority of these cells were located at muscle layer, and only a few were found in serosa. GFP+ cells were rarely observed in urothelium with E-cadherin staining, indicating that they did not differentiate into epithelial cells. The majority of GFP+ cells located at muscularis were strongly stained with an anti-vimentin antibody, indicating that they had differentiated into stromal cells and perivascular cells. GFP+ cells located in the endothelium were CD31+, indicating that they had differentiated into endothelial cells. Taken together, these results demonstrate that transplanted M-MSCs stably engrafted and migrated to the damaged muscular layer, where they differentiated into different cell types.

**Figure 6. Immunostaining analysis of transplanted M-MSCs.**

Confocal micrographs of M-MSCs stably expressing GFP (red) and immunostaining of the marker proteins E-cadherin (Ecad), vimentin, and CD31 (green) in bladder sections of DM-DUA + M-MSC rats at 7 DAT (magnification ×1,000, scale bar = 10 □m). Nuclei were stained with DAPI (blue). Arrows indicate GFP+ engrafted cells co-expressing each tissue marker. Notably, the majority of transplanted GFP+ cells at 7 DAT was strongly stained with the vimentin expressing stromal cells and perivascular cells.

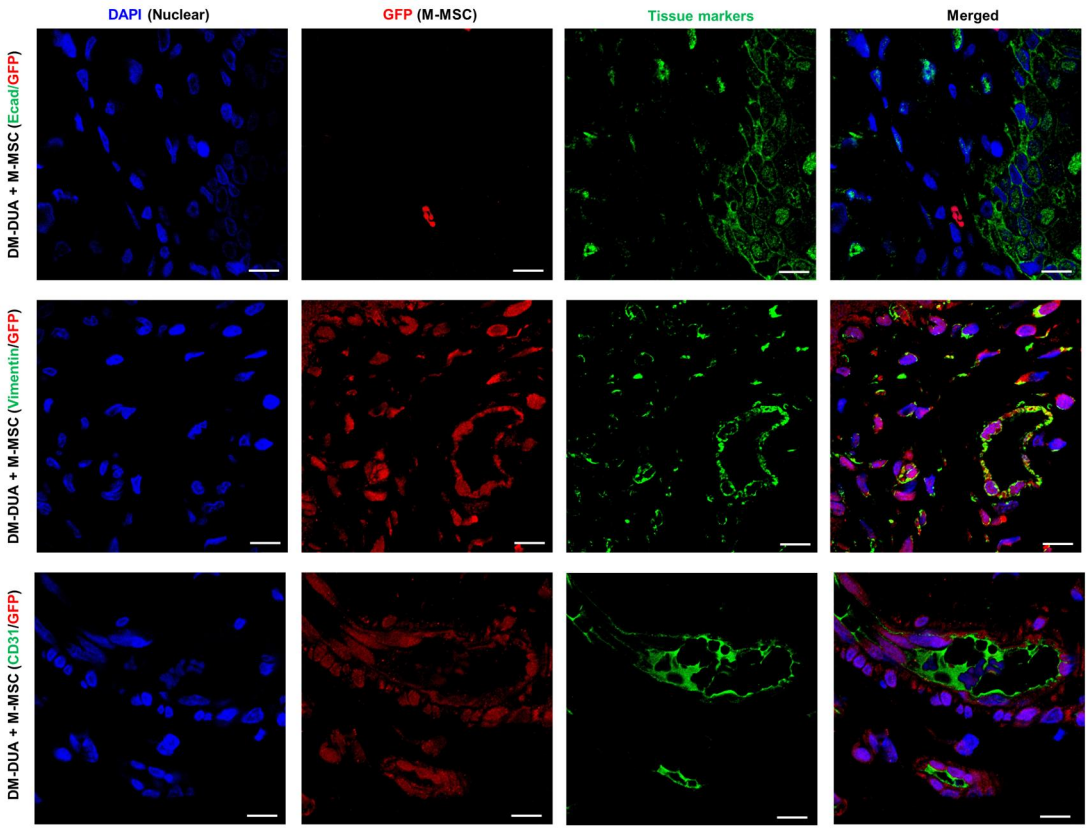

# DISCUSSION

In this present study, we made diabetic DUA model with STZ and evaluated therapeutic effect of M-MSC. Diabetic rats were with 50 mg/kg STZ had adequate survival rate and the optimal timing for stem cell injection was 21 days later. Diabetic models showed atrophy and apoptosis of detrusor smooth muscles in immunohistochemical staining and presented voiding profiles of DUA such as increased micturition interval, large post-void residual, impaired contractility and decreased micturition pressure. M-MSCs restored histological and functional changes of diabetic DUA rats.

To our knowledge, this is the first study to demonstrate therapeutic effect of M-MSCs in diabetic DUA model. In the previous study by Zhang et al, autologous adipose tissue derived mesenchymal stem cells (ADSCs, $3.0x10^6$ cells) were injected via tail vein or directly to bladder. ADSCs ameliorated diabetic bladder dysfunction significantly, but there was no significant difference in therapeutic efficacy based on the route of stem cell injection.[27] In addition, they suggested that defocused low-energy shock wave recruited endogenous stem cells by secreting more NGF and VEGF.[28] Our diabetic model used a

lower dose of M-MSCs from human embryo and injection route was direct transplantation to bladder serosa accordingly to our previous study protocols in IC rat model.

The advantage of hESCs is that hESCs can differentiate to all cells types of the body upon proper induction without losing pluripotency.[29,30] However, one major concern is a possibility for rejection via antigenicity and immunological processes. T cells and major histocompatibility complex class 1 (MHC-1) are considered to have a pivotal role in xenorejection of hESCs and their derivatives.[31] However, previous studies identified the immune-stimulatory capacity of cells is very low.[32] Using mice that were conditioned to carry peripheral blood leukocytes from human origin to test human leukocyte alloresponse toward undifferentiated and differentiated hESCs, only a minute immune response was detected.[33]

Hyperglycemia can induce cellular damages through oxidative stress and other mechanisms. Excess glucose oxidation produces electrons used in the formation of reactive oxygen species.[34] *In vitro* experimental studies with animal models showed functional changes in detrusor smooth muscle, neuronal impairment and urothelial dysfunction.[35] And the severity of diabetic cystopathy depends mainly on disease duration and controllability.

Our diabetic DUA rat model is presumed to have predominant myogenic pathophysiology. DUA profile became apparent 21 days after induction with increased smooth muscle atrophy and apoptosis leading to decreased detrusor contractility whereas no difference in neurofilament was observed. However, suggested mechanisms of diabetic cystopathy not only includes myogenic degeneration but also denervation. Considering acontractile bladder observed in 28 days after induction, prolonged duration of diabetic state might have led to a more irreversible state of bladder damage including denervation. Longitudinal changes in histology of diabetic rat bladder should be determined whether models with prolonged diabetes present decreased neurofilament (NGF) and angiogenesis (VEGF).

Previously, we have demonstrated that transplanted M-MSCs replenish denuded urothelium in early stage and progressively contribute to perivascular cells in IC rat models. The exact mechanism for bladder function restoration of our model is unclear, but histological change suggests that M-MSCs might have ameliorated smooth muscle apoptosis and differentiated into myogenic structures and pericytes near vessel-like structures in muscular

layer. Regeneration of damaged myocytes resulted in restored detrusor contractility. However, additional GFP staining for smooth muscle (alpha smooth-muscle actin) and PCR of gene expression is needed.

The limitation of our study is that we only utilized one means to induce diabetic state. Diabetes can be generally classified as type 1 diabetes -inability to produce enough insulin due to loss of insulin-producing β–cells in pancreas islets and type 2 diabetes- cells non-respondent to insulin leading to reduction in uptake of sugars from blood stream. STZ is toxic to β–cells in pancreas and induces type 1 diabetes. In addition, most of DM patients have type 2 diabetes which have multifactorial etiologies including genetics, environment, diet and autoimmune.[36] However, as hyperglycemia is the principal factor in pathogenesis and natural course of diabetes, so animal models of both type 1 and type 2 are extensively used for further investigation of DM.

Further studies with our current model are planned in following orders; 1) additional organ bath studies with carbachol (Cch) and 1 mM ATP to demonstrate that diminished detrusor contractility in DM model is restored with M-MSCs. 2) Additional GFP staining and

*in vivo* confocal imaging (confocal microscopy, microcystoscopy and micro-PET) to identify what M-MSCs differentiate into, how long transplanted M-MSCs are sustained and their potential tumorigenicity. 3) PCR of genes associated with smooth muscle apoptosis to figure out the exact pathogenesis of our diabetic DUA and mechanisms of restoration by M-MSCs.

# CONCLUSION

Effective therapeutic strategies for detrusor underactivity is limited. In this present study, we established our own diabetic DUA model with single injection of STZ in rat. Our rat model presented voiding parameters similar to those of underactive bladder patients; low maximal flow rate, low detrusor pressure, and large post-void residual etc. In addition, single injection of M-MSC has proven its therapeutic efficacy by restoring histological abnormalities and abnormal voiding patterns. The exact pathophysiology and therapeutic mechanisms of M-MSC are unclear. Further studies to reveal the mechanisms of effectiveness with M-MSCs is needed.

# REFERENCE


1. Abrams P, Cardozo L, Fall M et al: The standardisation of terminology in lo wer urinary tract function: report from the standardisation sub-committee of t he International Continence Society. Urology 2003; **61:** 37.
2. Aldamanhori R, Chapple CR: Underactive bladder, detrusor underactivity, defi nition, symptoms, epidemiology, etiopathogenesis, and risk factors. Curr Opin Urol 2017; **27:** 293.
3. Gammie A, Kaper M, Dorrepaal C et al: Signs and Symptoms of Detrusor Underactivity: An Analysis of Clinical Presentation and Urodynamic Tests Fr om a Large Group of Patients Undergoing Pressure Flow Studies. Eur Urol 2016; **69:** 361.
4. Chapple CR, Osman NI, Birder L et al: The underactive bladder: a new clin ical concept? Eur Urol 2015; **68:** 351.
5. van Koeveringe GA, Vahabi B, Andersson KE et al: Detrusor underactivity: a plea for new approaches to a common bladder dysfunction. Neurourol Uro dyn 2011; **30:** 723.
6. Cucchi A, Quaglini S and Rovereto B: Development of idiopathic detrusor u nderactivity in women: from isolated decrease in contraction velocity to obvi ous impairment of voiding function. Urology 2008; **71:** 844.
7. Osman NI, Chapple CR: Contemporary concepts in the aetiopathogenesis of detrusor underactivity. Nat Rev Urol 2014; **11:** 639.
8. Osman N, Mangera A, Hillary C et al: The underactive bladder: detection an d diagnosis. F1000Res 2016; **5**.
9. Osman NI, Chapple CR, Abrams P et al: Detrusor underactivity and the und eractive bladder: a new clinical entity? A review of current terminology, defi nitions, epidemiology, aetiology, and diagnosis. Eur Urol 2014; **65:** 389.
10. Zimmet P, Alberti KG, Magliano DJ et al: Diabetes mellitus statistics on pre valence and mortality: facts and fallacies. Nat Rev Endocrinol 2016; **12:** 616.
11. Yuan Z, Tang Z, He C et al: Diabetic cystopathy: A review. J Diabetes 201

5; **7:** 442.

12. Arrellano-Valdez F, Urrutia-Osorio M, Arroyo C et al: A comprehensive revie w of urologic complications in patients with diabetes. Springerplus 2014; **3:** 549.
13. Liu G, Li M, Vasanji A et al: Temporal diabetes and diuresis-induced alterati on of nerves and vasculature of the urinary bladder in the rat. BJU Int 2011; **107:** 1988.
14. Deli G, Bosnyak E, Pusch G et al: Diabetic neuropathies: diagnosis and man agement. Neuroendocrinology 2013; **98:** 267.
15. Tarcan T, Rademakers K, Arlandis S et al: Do the definitions of the underac tive bladder and detrusor underactivity help in managing patients: Internationa l Consultation on Incontinence Research Society (ICI-RS) Think Tank 2017? Neurourol Urodyn 2018; **37:** S60.
16. Osman NI, Esperto F and Chapple CR: Detrusor Underactivity and the Unde ractive Bladder: A Systematic Review of Preclinical and Clinical Studies. Eur Urol 2018; **74:** 633.
17. Thomas AW, Cannon A, Bartlett E et al: The natural history of lower urinar y tract dysfunction in men: minimum 10-year urodynamic follow-up of untre ated bladder outlet obstruction. BJU Int 2005; **96:** 1301.
18. Ratajczak MZ, Machalinski B, Wojakowski W et al: A hypothesis for an em bryonic origin of pluripotent Oct-4(+) stem cells in adult bone marrow and o ther tissues. Leukemia 2007; **21:** 860.
19. Kim JH, Lee SR, Song YS et al: Stem cell therapy in bladder dysfunction: where are we? And where do we have to go? Biomed Res Int 2013; **2013:** 930713.
20. Kim A, Yu HY, Heo J et al: Mesenchymal stem cells protect against the tiss ue fibrosis of ketamine-induced cystitis in rat bladder. Sci Rep 2016; **6:** 308 81.
21. Kim A, Yu HY, Lim J et al: Improved efficacy and in vivo cellular properti es of human embryonic stem cell derivative in a preclinical model of bladde

r pain syndrome. Sci Rep 2017; **7:** 8872.

22. Song M, Lim J, Yu HY et al: Mesenchymal Stem Cell Therapy Alleviates I nterstitial Cystitis by Activating Wnt Signaling Pathway. Stem Cells Dev 201 5; **24:** 1648.
23. Golbidi S, Laher I: Bladder dysfunction in diabetes mellitus. Front Pharmacol 2010; **1:** 136.
24. Aizawa N, Igawa Y: Pathophysiology of the underactive bladder. Investig Cli n Urol 2017; **58:** S82.
25. Kim JM, Hong KS, Song WK et al: Perivascular Progenitor Cells Derived F rom Human Embryonic Stem Cells Exhibit Functional Characteristics of Peric ytes and Improve the Retinal Vasculature in a Rodent Model of Diabetic Ret inopathy. Stem Cells Transl Med 2016; **5:** 1268.
26. Hong KS, Bae D, Choi Y et al: A porous membrane-mediated isolation of mesenchymal stem cells from human embryonic stem cells. Tissue Eng Part C Methods 2015; **21:** 322.
27. Zhang H, Qiu X, Shindel AW et al: Adipose tissue-derived stem cells ameli orate diabetic bladder dysfunction in a type II diabetic rat model. Stem Cells Dev 2012; **21:** 1391.
28. Jin Y, Xu L, Zhao Y et al: Endogenous Stem Cells Were Recruited by Defo cused Low-Energy Shock Wave in Treating Diabetic Bladder Dysfunction. Ste m Cell Rev 2017; **13:** 287.
29. Thomson JA, Itskovitz-Eldor J, Shapiro SS et al: Embryonic stem cell lines derived from human blastocysts. Science 1998; **282:** 1145.
30. Itskovitz-Eldor J, Schuldiner M, Karsenti D et al: Differentiation of human e mbryonic stem cells into embryoid bodies compromising the three embryonic germ layers. Mol Med 2000; **6:** 88.
31. Jurisicova A, Casper RF, MacLusky NJ et al: HLA-G expression during prei mplantation human embryo development. Proc Natl Acad Sci U S A 1996; **9 3:** 161.
32. de Almeida PE, Ransohoff JD, Nahid A et al: Immunogenicity of pluripotent

stem cells and their derivatives. Circ Res 2013; **112:** 549.

33. Drukker M, Katchman H, Katz G et al: Human embryonic stem cells and th eir differentiated derivatives are less susceptible to immune rejection than adu lt cells. Stem Cells 2006; **24:** 221.

34. Liu G, Daneshgari F: Diabetic bladder dysfunction. Chin Med J (Engl) 2014; **127:** 1357.

35. Wittig L, Carlson KV, Andrews JM et al: Diabetic bladder dysfunction: A re view. Urology 2018, doi: 10.1016/j.urology.2018.10.010.

36. Furman BL: Streptozotocin-Induced Diabetic Models in Mice and Rats. Curr Protoc Pharmacol 2015; **70:** 5.47.1.

# 국문요약

저활동성 방광은 방광 충만 감각의 상실, 배뇨근 수축 저하로 인한 불충분한 방광 배출을 특징으로 하는 증상으로 현재 약물 혹은 수술적 치료는 제한적이다. 노화, 당뇨, 신경학적 질환, 약물, 감염 등 다양한 위험인자가 있고 이 중 당뇨는 그 유병률이 10%에 이를 정도로 전세계적으로 중요한 질환이다. 당뇨의 합병증은 매우 다양하며 이 중, 당뇨성 방광병증은 질병의 심한 정도, 지속 기간 및 조절 여부에 따라 그 정도가 다를 수 있으나 최대 50%의 당뇨 환자에서 나타날 수 있다고 알려져 있다. 본 연구는 쥐에서 당뇨병성 방광 기능 저하모델을 구축하고 인간 배아 줄기세포로부터 유래한 중간엽 줄기세포 주입의 치료 효과를 확인하고자 하였다.

생후 8주 된 암컷 Sprague Dawley rat과 인간배아 줄기세포로부터 분화한 중간엽 줄기세포를 사용하였다. 쥐는 12시간 이상 금식 후 streptozotocin (STZ) 50mg/kg를 복강 내 1회 주입하였다. 3일 후 꼬리에서 혈당을 확인, 200mg/dL이 넘는 경우만 당뇨쥐로 정의, 본 연구에 포함하였다. 당뇨 유발 3주 후 총 50

마리의 쥐를 다섯 집단으로 나누어 줄기세포 주입을 시행하였다. (대조군 10마리, 당뇨군 10마리, 250k 줄기세포 주입군 10마리, 500k 줄기세포 주입군 10마리, 1,000k 줄기세포 주입군 10마리) 줄기세포는 26게이지 바늘을 통해 직접 방광의 전벽부의 점막 하 층에 주입하였다. 줄기세포 주입 1주일 후, 각성 상태의 방광 기능 평가와 면역조직화학염색을 시행하였다.

당뇨군은 대조군에 비해 배뇨 간격이 길고 배뇨근의 압력이 낮고 배뇨 후 잔뇨량이 많았으며 면역조직화학염색에서 근육세포의 감소와 자멸을 보였다. 줄기세포는 주입한 모든 용량에서 방광 기능 부전과 조직학적 변성을 완화시켰으며 주로 방광 근육층의 근육세포와 혈관 주위 세포에서 관찰되었다.

본 연구를 통하여 STZ 주입을 통하여 당뇨성 방광 저활동 쥐 모델을 성공적으로 만들었다. 또한 본 모델에서 인간 배아 줄기세포로부터 유래한 중간엽 줄기세포 주입의 치료 효과를 확인할 수 있었다. 줄기세포의 분화와 그 치료 효과에 대한 추가 연구가 심도 있게 진행되어야 할 것이다.